

hep-ph/0312262

CERN-TH/2003-310

UMN-TH-2225/03

FTPI-MINN-03/37

## Gravitino Dark Matter in the CMSSM

John Ellis<sup>1</sup>, Keith A. Olive<sup>2</sup>, Yudi Santoso<sup>2</sup> and Vassilis C. Spanos<sup>2</sup>

<sup>1</sup>*TH Division, CERN, Geneva, Switzerland*

<sup>2</sup>*William I. Fine Theoretical Physics Institute,  
University of Minnesota, Minneapolis, MN 55455, USA*

### Abstract

We consider the possibility that the gravitino might be the lightest supersymmetric particle (LSP) in the constrained minimal extension of the Standard Model (CMSSM). In this case, the next-to-lightest supersymmetric particle (NSP) would be unstable, with an abundance constrained by the concordance between the observed light-element abundances and those calculated on the basis of the baryon-to-entropy ratio determined using CMB data. We modify and extend previous CMSSM relic neutralino calculations to evaluate the NSP density, also in the case that the NSP is the lighter stau, and show that the constraint from late NSP decays is respected only in a limited region of the CMSSM parameter space. In this region, gravitinos might constitute the dark matter.

CERN-TH/2003-310

December 2003

# 1 Introduction

If  $R$  parity is conserved, the lightest supersymmetric particle (LSP) is stable, and a possible candidate for the cold dark matter postulated by astrophysicists and cosmologists [1]. Most analyses of such supersymmetric dark matter have assumed that the LSP is the partner of some combination of Standard Model particles, such as the lightest neutralino  $\chi$ , with an abundance calculated from the freeze-out of annihilation processes in a thermal initial state. However, another generic possibility is that the LSP is the gravitino  $\tilde{G}$  [2] - [8], whose relic abundance would get contributions from the decays of the next-to-lightest supersymmetric particle (NSP) and possibly other mechanisms.

As we discuss in more detail below, the lifetime of the NSP is typically such that it decays between Big-Bang nucleosynthesis (BBN) and the ‘re-’ combination process when the cosmic microwave background (CMB) was released from matter. Since NSP decays release entropy during this epoch, they are constrained by the concordance of the observed light-element abundances with BBN calculations assuming the baryon-to-entropy ratio inferred from CMB observations. For a typical lifetime  $\tau_{NSP} = 10^8$  s, the observed  ${}^6\text{Li}$  abundance implies [9]

$$\frac{n_{NSP}}{n_\gamma} < 5 \times 10^{-14} \left( \frac{100 \text{ GeV}}{m_{NSP}} \right) \quad (1)$$

before NSP decay, with the D/H ( ${}^4\text{He}$ ) abundance providing a constraint which is weaker by a factor of about 10 (20). Assuming a baryon-to-entropy ratio  $\eta \equiv n_B/n_\gamma = 6.0 \times 10^{-10}$ , in agreement with the WMAP result  $\eta = 6.1_{-0.2}^{+0.3} \times 10^{-10}$  [10], (1) implies the constraint  $n_{NSP}/n_B < 10^{-4}(100 \text{ GeV}/m_{NSP})$  before the onset of NSP decay. To assess the power of this constraint, we re-express it in terms of  $\Omega_{NSP}^0 h^2$ , the relic density that the NSP *would have* today, *if* it had not decayed:

$$\Omega_{NSP}^0 h^2 < 10^{-2} \Omega_B h^2 \simeq 2 \times 10^{-4}, \quad (2)$$

where  $\Omega_B h^2 \simeq 2 \times 10^{-2}$  is the present-day baryon density. However, the requirement (2) would be relaxed for a shorter-lived NSP [7], as we discuss later.

In contrast, assuming that the lightest neutralino  $\chi$  is the LSP, there have been many calculations of  $\Omega_\chi h^2$  in the constrained minimal supersymmetric extension of the Standard Model (CMSSM), in which the GUT-scale input gaugino masses  $m_{1/2}$  and scalar masses  $m_0$  are each assumed to be universal [11, 12, 13, 14]. These calculations find generic strips of CMSSM parameter space in which

$$\Omega_\chi h^2 \sim 5 \times \Omega_B h^2 \sim 0.1 \quad (3)$$

This is similar to the range of the cold dark matter density  $\Omega_{CDM}h^2$  favoured by astrophysicists and cosmologists, which is one reason why neutralino dark matter has been quite popular.

In this paper, we assume no *a priori* relation between  $m_{3/2}$  and the soft supersymmetry-breaking masses  $m_{1/2}$  and  $m_0$  of the spartners of Standard Model particles in the CMSSM. This is possible in, e.g., the framework of  $N = 1$  supergravity with a non-minimal Kähler potential [15]. In such a framework, the LSP might well be the gravitino  $\tilde{G}$ . In this case, the NSP would likely be the lightest supersymmetric partner of some combination of Standard Model particles, such as the lightest neutralino  $\chi$  or the lighter stau  $\tilde{\tau}_1$ . Particularly in the  $\chi$  NSP case, one might expect  $\Omega_{NSP}^0 h^2$  to be near the range (3). Comparing this with the condition (2) necessary for gravitino dark matter, we see that, if  $\tau_{NSP} = 10^8$  s, gravitino dark matter could be possible only in rather different regions of the CMSSM parameter space, where the NSP density is very suppressed compared with the usual  $\chi$  density. Moreover, in this case, NSP decays alone could not provide enough gravitinos, since they could only yield  $\Omega_{3/2} h^2 < \Omega_{NSP}^0 h^2$ , so there would need to be some supplementary mechanism for producing gravitinos, if they were to provide all the cold dark matter. For example, gravitino production during reheating after inflation could produce a sufficient abundance of gravitinos if the reheat temperature is relatively large,  $\sim \mathcal{O}(10^{10})$  GeV [7].

The first step in our exploration of the gravitino dark matter possibility is to calculate  $\Omega_{NSP}^0 h^2$  throughout the  $(m_{1/2}, m_0)$  planes for different choices of  $\tan \beta$  and the sign of  $\mu$  in the CMSSM, assuming that the trilinear soft supersymmetry-breaking parameter  $A_0 = 0$ . In the regions where  $m_\chi < m_{\tilde{\tau}_1}$ , this is essentially equivalent to the usual neutralino dark matter density calculation. However, as we discuss below, this calculation must be adapted in the region where  $m_{\tilde{\tau}_1} < m_\chi$ . Moreover, one must take into account the possibility of a cosmological  $\tilde{\tau}_1$  asymmetry, in which case the relic  $\tilde{\tau}_1$  density would be larger than that given by the standard freeze-out calculation. We next compute the NSP lifetime and use the detailed constraints from the abundances of the light elements as computed in (1) for fixed  $\eta = 6 \times 10^{-10}$ . This allows us to delineate the regions of the CMSSM  $(m_{1/2}, m_0)$  planes where gravitino dark matter appears possible. We find limited regions of the  $(m_{1/2}, m_0)$  planes that are allowed. In these regions, the density of relic gravitinos due to NSP decay is typically less than the range favoured by astrophysics and cosmology. As noted above, supplementary mechanisms for gravitino production, such as thermal production in the early Universe, might then enable gravitinos to constitute the cold dark matter.

## 2 NSP Density Calculations

In the framework of the CMSSM with a light gravitino discussed here, the candidates for the NSP are the lightest partners of Standard Model particles. In generic regions of CMSSM parameter space, these are the lightest neutralino  $\chi$  and the lighter stau  $\tilde{\tau}_1$ <sup>1</sup>. In regions where  $\chi$  is the NSP, the calculation of the NSP density  $\Omega_{NSP}^0 h^2$  is identical with that of  $\Omega_{LSP} h^2$  in the CMSSM with a heavier gravitino, and we can recycle standard results.

Extending these calculations of  $\Omega_{NSP}^0 h^2$  to regions where the  $\tilde{\tau}_1$  is the NSP requires some modifications. Whereas the Majorana  $\chi$  is its own antiparticle, one must distinguish between the  $\tilde{\tau}_1$  and its antiparticle  $\tilde{\tau}_1^*$ , and calculate the sum of their relic densities. This requires a careful accounting of the statistical factors in all relevant annihilation and coannihilation processes. We have also made a careful treatment of the regions where there is rapid  $\tilde{\tau}_1 - \tilde{\tau}_1^*$  annihilation via Higgs poles, and a non-relativistic expansion in powers of the NSP velocity is inadequate. Here our treatment follows that of the neutralino LSP case in [17, 11, 13].

It is important to note that one would, in general, expect a net  $\tilde{\tau}_1$  asymmetry  $\eta_{\tilde{\tau}_1} \equiv \lambda \eta_B$ , where  $\lambda \sim O(1)$ . This would be the expectation, for example, in leptogenesis scenarios, and would also appear in other baryogenesis scenarios, as a result of electroweak sphalerons. However, in the context of the MSSM, there exist  $\tilde{\tau}_1 \tilde{\tau}_1 \rightarrow \tau\tau$  annihilation processes which would dilute any existing lepton asymmetry stored in the  $\tilde{\tau}$  sleptons, and the final relic density is given by the calculation described above.

## 3 NSP Decays

Using the standard  $N = 1$  supergravity Lagrangian [18, 19], one can calculate the rates for the various decay channels of candidate NSPs to gravitinos.

The dominant decay of a  $\chi$  NSP would be into a gravitino and a photon, for which we calculate the width

$$\Gamma_{\chi \rightarrow \tilde{G} \gamma} = \frac{1}{16\pi} \frac{C_{\chi\gamma}^2}{M_P^2} \frac{m_\chi^5}{m_{3/2}^2} \left(1 - \frac{m_{3/2}^2}{m_\chi^2}\right)^3 \left(\frac{1}{3} + \frac{m_{3/2}^2}{m_\chi^2}\right) \quad (4)$$

where  $C_{\chi\gamma} = (O_{1\chi} \cos \theta_W + O_{2\chi} \sin \theta_W)$  and  $O$  is the neutralino diagonalization matrix,  $O^T \mathcal{M}_N O = \mathcal{M}_N^{diag}$ . Note that in this and the following equations  $M_P \equiv 1/\sqrt{8\pi G_N}$ .

---

<sup>1</sup>The lighter stop could also be the NSP if the trilinear coupling  $A_0$  is large [16], but here we fix  $A_0 = 0$  for simplicity.

A  $\chi$  NSP may also decay into a gravitino and a  $Z$  boson, for which we calculate the rate

$$\begin{aligned}\Gamma_{\chi \rightarrow \tilde{G} Z} &= \frac{1}{16\pi} \frac{C_{\chi Z}^2}{M_P^2} \frac{m_\chi^5}{m_{3/2}^2} \mathcal{F}(m_\chi, m_{3/2}, M_Z) \\ &\times \left\{ \left(1 - \frac{m_{3/2}^2}{m_\chi^2}\right)^2 \left(\frac{1}{3} + \frac{m_{3/2}^2}{m_\chi^2}\right) - \frac{M_Z^2}{m_\chi^2} \mathcal{G}(m_\chi, m_{3/2}, M_Z) \right\}\end{aligned}\quad (5)$$

where  $C_{\chi Z} = (-O_{1\chi} \sin \theta_W + O_{2\chi} \cos \theta_W)$ , and we use the auxiliary functions

$$\mathcal{F}(m_\chi, m_{3/2}, M_Z) = \left[ \left(1 - \left(\frac{m_{3/2} + M_Z}{m_\chi}\right)^2\right) \left(1 - \left(\frac{m_{3/2} - M_Z}{m_\chi}\right)^2\right) \right]^{1/2}, \quad (6)$$

$$\mathcal{G}(m_\chi, m_{3/2}, M_Z) = 1 + \frac{m_{3/2}^3}{m_\chi^3} \left(4 + \frac{m_{3/2}}{3m_\chi}\right) + \frac{M_Z^4}{3m_\chi^4} - \frac{M_Z^2}{m_\chi^2} \left(1 - \frac{m_{3/2}^2}{3m_\chi^2}\right). \quad (7)$$

Note that in the limit  $M_Z \rightarrow 0$  we obtain  $\Gamma_{\chi \rightarrow \tilde{G} Z} \rightarrow \Gamma_{\chi \rightarrow \tilde{G} \gamma}$  by replacing  $C_{\chi Z}$  with  $C_{\chi \gamma}$ .

Decays of a  $\chi$  NSP into a gravitino and a Higgs boson are also possible, with a rate

$$\begin{aligned}\Gamma_{\chi \rightarrow \tilde{G} h} &= \frac{1}{64\pi} \frac{C_{\chi h}^2}{M_P^2} \frac{m_\chi^5}{m_{3/2}^2} \mathcal{F}(m_\chi, m_{3/2}, m_h) \\ &\times \left\{ \left(1 - \frac{m_{3/2}^2}{m_\chi^2}\right)^2 \left(\frac{1}{3} + \frac{m_{3/2}^2}{m_\chi^2}\right) - \frac{m_h^2}{m_\chi^2} \mathcal{H}(m_\chi, m_{3/2}, m_h) \right\}\end{aligned}\quad (8)$$

where  $C_{\chi h} = (O_{4\chi} \cos \alpha - O_{3\chi} \sin \alpha)$  and

$$\mathcal{H}(m_\chi, m_{3/2}, m_h) = 1 - \frac{m_h^2}{m_\chi^2} + \frac{1}{3m_\chi^4} (m_{3/2}^4 + m_{3/2}^2 m_h^2 + m_h^4). \quad (9)$$

Analogously, for the heavy Higgs boson  $H$  we get  $\Gamma_{\chi \rightarrow \tilde{G} h} \rightarrow \Gamma_{\chi \rightarrow \tilde{G} H}$  by replacing  $C_{\chi h}$  with  $C_{\chi H} \equiv (O_{4\chi} \sin \alpha + O_{3\chi} \cos \alpha)$ , and  $m_h$  with  $m_H$ . The corresponding formula for  $\chi \rightarrow \tilde{G} + A$ , where  $A$  is the CP-odd Higgs boson in the MSSM, is also given by (9), but with  $m_h$  replaced by  $m_A$  and  $C_{\chi h} \rightarrow C_{\chi A} \equiv (O_{4\chi} \cos \beta + O_{3\chi} \sin \beta)$ .

Finally, the dominant decay of a  $\tilde{\tau}$  NSP would be into a gravitino and a  $\tau$ , with the rate:

$$\Gamma_{\tilde{\tau} \rightarrow \tilde{G} \tau} = \frac{1}{48\pi} \frac{1}{M_P^2} \frac{m_{\tilde{\tau}}^5}{m_{3/2}^2} \left(1 - \frac{m_{3/2}^2}{m_{\tilde{\tau}}^2}\right)^4. \quad (10)$$

where we have neglected the  $O(m_\tau^2/m_{\tilde{\tau}}^2)$  terms.

## 4 Effects of Gravitino Decay Products on Light-Element Abundances

The effects of electromagnetic shower development between Big-Bang Nucleosynthesis (BBN) and ‘re-’combination have been well studied, most recently in [9], where the simplest case of  $\chi \rightarrow \tilde{G} + \gamma$  decays were considered. The late injection of electromagnetic energy can wreak havoc on the abundances of the light elements. Energetic photons may destroy deuterium, destroy  ${}^4\text{He}$  (which may lead to excess production of D/H), destroy  ${}^7\text{Li}$ , and/or overproduce  ${}^6\text{Li}$ . The concordance between BBN calculations and the observed abundances of these elements can be used to derive a limit on the density of any decaying particle. In general, this limit will depend on both the baryon asymmetry  $\eta_B$ , which controls the BBN predictions, and on the life-time of the decaying particle  $\tau_X$ . For a fixed value  $\eta_B = 6 \times 10^{-10}$ , as suggested by CMB observations, the bounds derived from Fig. 8(a) in [9] may be parameterized approximately as

$$y < 0.13 x^2 - 2.85 x + 3.16, \quad (11)$$

where  $y \equiv \log(\zeta_X/\text{GeV}) \equiv \log(m_X n_X/n_\gamma/\text{GeV})$  and  $x \equiv \log(\tau_X/\text{s})$ , for the electromagnetic decays of particles  $X$  with lifetimes  $10^{12} \text{ s} > \tau_{NSP} \gtrsim 10^4 \text{ s}$ . In our subsequent analysis we use the actual data corresponding to the limit in [9] in order to delineate the allowed regions of the  $(m_{1/2}, m_0)$  planes, but (11) may help the reader understand qualitatively our results.

The other NSP decay modes listed above inject electrons, muons and hadrons into the primordial medium, as well as photons. Electromagnetic showers develop similarly, whether they are initiated by electrons or photons, so we can apply the analysis of [9] directly also to electrons. Bottom, charm and  $\tau$  particles decay before they interact with the cosmological medium, so new issues are raised only by the interactions of muons, pions and strange particles. In fact, if the NSP lifetime exceeds about  $10^4 \text{ s}$ , these also decay before interacting, and the problem reduces to the purely electromagnetic case. In the case of a shorter-lived NSP, we would need to consider also hadronic interactions with the cosmological medium [20], which would strengthen the limits on gravitino dark matter that we derive below on the basis of electromagnetic showers alone. In the following, we do not consider regions of the  $(m_{1/2}, m_0)$  planes where  $\tau_{NSP} < 10^4 \text{ s}$ .

It is sufficient for our purposes to treat the decays of  $\mu$ ,  $\pi$  and  $K$  as if their energies were equipartitioned among their decay products. In this approximation, we estimate that the fractions of particle energies appearing in electromagnetic showers are  $\pi^0 : 100\%$ ,  $\mu : 1/3$ ,  $\pi^\pm : 1/4$ ,  $K^\pm : 0.3$ ,  $K^0 : 0.5$ . Using the measured decay branching ratios of the  $\tau$ , we then estimate that  $\sim 0.3$  of its energy also appears in electromagnetic showers. In the case of

generic hadronic showers from  $Z$  or Higgs decay, we estimate that  $\sim 0.6$  of the energy is electromagnetic, due mainly to  $\pi^0$  and  $\pi^\pm$  production.

Our procedure is then as follows. First, on the basis of a freeze-out calculation, we calculate the NSP relic density  $\Omega_X^0 h^2 = 3.9 \times 10^7 \text{ GeV}^{-1} \zeta_X$ . Next, we use the calculated life-time  $\tau_X$  to compute the ratio of the relic density to the limiting value,  $\zeta_X^{CEFO}$  provided by the analysis of [9], taking into account the electromagnetic energy decay fractions estimated above. Finally, we require

$$r \equiv \frac{\zeta_X}{\zeta_X^{CEFO}} < 1. \quad (12)$$

## 5 Results

As compared to the case of CMSSM dark matter usually discussed, in the case of gravitino dark matter one must treat  $m_{3/2}$  as an additional free parameter, unrelated *a priori* to  $m_0$  and  $m_{1/2}$ . We incorporate the LEP constraint on  $m_h$  in the same way as in [13]<sup>2</sup>, and it appears as a nearly vertical (red) dot-dashed line in each of the following figures. Regions excluded by measurements of  $b \rightarrow s\gamma$  are shaded dark (green). For reference, the figures also display the strips of the  $(m_{1/2}, m_0)$  planes where  $0.094 < \Omega_{NSP}^0 < 0.129$ . This density is the same as  $\Omega_{LSP} h^2$  in a standard CMSSM analysis with a heavy gravitino, extended to include the unphysical case where the  $\tilde{\tau}_1$  is the LSP. We note the familiar ‘bulk’ regions and coannihilation ‘tails’, as well as rapid-annihilation ‘funnels’ for large  $\tan \beta$  [21, 17]. If these figures were extended to larger  $m_0$ , there would also be ‘focus-point’ regions [22, 23].

We now summarize our principal results, describing the interplay of these constraints with those associated specifically with gravitino dark matter, studying the  $(m_{1/2}, m_0)$  planes for three choices of  $\tan \beta$  and the sign of  $\mu$ : (1)  $\tan \beta = 10$ ,  $\mu > 0$ , (2)  $\tan \beta = 35$ ,  $\mu < 0$ , and (3)  $\tan \beta = 50$ ,  $\mu > 0$ . In each case, we consider four possibilities for  $m_{3/2}$ : two fixed values 10 GeV and 100 GeV, and two fixed ratios relative to  $m_0$ :  $m_{3/2} = 0.2 m_0$  and  $m_0$  itself. If  $m_{3/2} \gg m_0$ , the  $\tilde{G}$  is typically not the LSP, and this role is played by the lightest neutralino  $\chi$ , as assumed in most analyses of the CMSSM. In each  $(m_{1/2}, m_0)$  plane, we display as a (purple) dashed line the limit where the density of relic gravitinos from NSP decay becomes equal to the highest cold dark matter density allowed by WMAP and other data at the  $2\text{-}\sigma$  level, namely  $\Omega_{3/2} h^2 < 0.129$ : only regions below and to the right of this contour are allowed in our analysis.

---

<sup>2</sup>For simplicity, we do not show the LEP constraints on  $m_{\chi^\pm}$  and  $m_{\tilde{e}}$ , which do not impinge on the regions of parameters allowed by other constraints.

Fig. 1 displays the  $(m_{1/2}, m_0)$  planes for  $\tan\beta = 10$  and  $\mu > 0$ <sup>3</sup>. Panel (a) displays the choice  $m_{3/2} = 10$  GeV, in which case the LSP is the  $\tilde{G}$  throughout the displayed region of the  $(m_{1/2}, m_0)$  plane. Above and to the left of the (purple) dashed line, the relic density  $\Omega_{3/2}h^2$  of gravitinos yielded by NSP decay exceeds the  $2\text{-}\sigma$  upper limit on the cold dark matter density, 0.129, imposed by WMAP and other cosmological data. This region is therefore excluded. In the regions below the (purple) dashed line, the relic  $\tilde{G}$  density might be increased so as to provide the required cold dark matter density if there were significant thermal gravitino production, in addition to that yielded by NSP decay.

The light-element constraint on NSP decays is shown as the light (khaki) solid line corresponding to  $r = 1$ , where  $r$  is defined in (12). Regions to the right and below this line are allowed by this constraint. Here, and in the remaining figures below, the region which satisfies the abundance constraint is labelled  $r < 1$ . There is a solid (black) line with  $m_{1/2} \sim 800$  GeV which indicates where  $\tau_{NSP} = 10^4$  s. To the right of this line,  $\tau_{NSP} < 10^4$  s, the case we do not consider here because additional constraints due to hadronic decays must be included, so this region is left blank<sup>4</sup>.

We see that there is an extended strip between the grey (khaki) solid line and the solid (black) line. This strip is truncated above  $m_0 \simeq 650$  GeV, because the relic density of gravitinos from NSP decay becomes too large. This is true up to  $\sim 2900$  GeV, where the relic density drops as we approach the focus-point region. Here a small allowed region opens up as the  $r = 1$  curve bends towards lower values of  $m_{1/2}$ . The allowed strip broadens in the low- $m_0$  region where  $m_{\tilde{\tau}_1} < m_\chi$ , below the dotted (red) line where  $m_\chi = m_{\tilde{\tau}_1}$ . In this region, gravitino dark matter is permitted.

Turning now to panel (b) of Fig. 1, where the choice  $m_{3/2} = 100$  GeV is made, we see a near-vertical black line at  $m_{1/2} \sim 250$  GeV: the gravitino is the LSP only to its right. The  $\tau_{NSP} = 10^4$  s line has disappeared to larger  $m_{1/2}$ , and is not shown. In this case the  $\Omega_{3/2}h^2$  constraint is much more important than in panel (a), forcing  $m_0$  to be relatively small, simply because  $m_{3/2}$  is larger. The only region allowed by the light-element constraint on NSP decays is in the bottom right-hand corner, in the region where the  $\tilde{\tau}_1$  is the NSP.

In panel (c) of Fig. 1, for  $m_{3/2} = 0.2m_0$ , there is also a black line to whose right the  $\tilde{G}$  is the LSP, which is now diagonal, and the  $\Omega_{3/2}h^2$  constraint is similar to that in panel (b). Most of the region allowed by the light-element constraint on NSP decays is in the region where the  $\tilde{\tau}_1$  is the NSP, though a sliver of parameter space runs above the dotted curve.

---

<sup>3</sup>The case  $\tan\beta = 10$  and  $\mu < 0$  is very similar, with the exception that the  $b \rightarrow s\gamma$  constraint is more important.

<sup>4</sup>This line would disappear to larger  $m_{1/2}$  already for  $m_{3/2} = 20$  GeV.



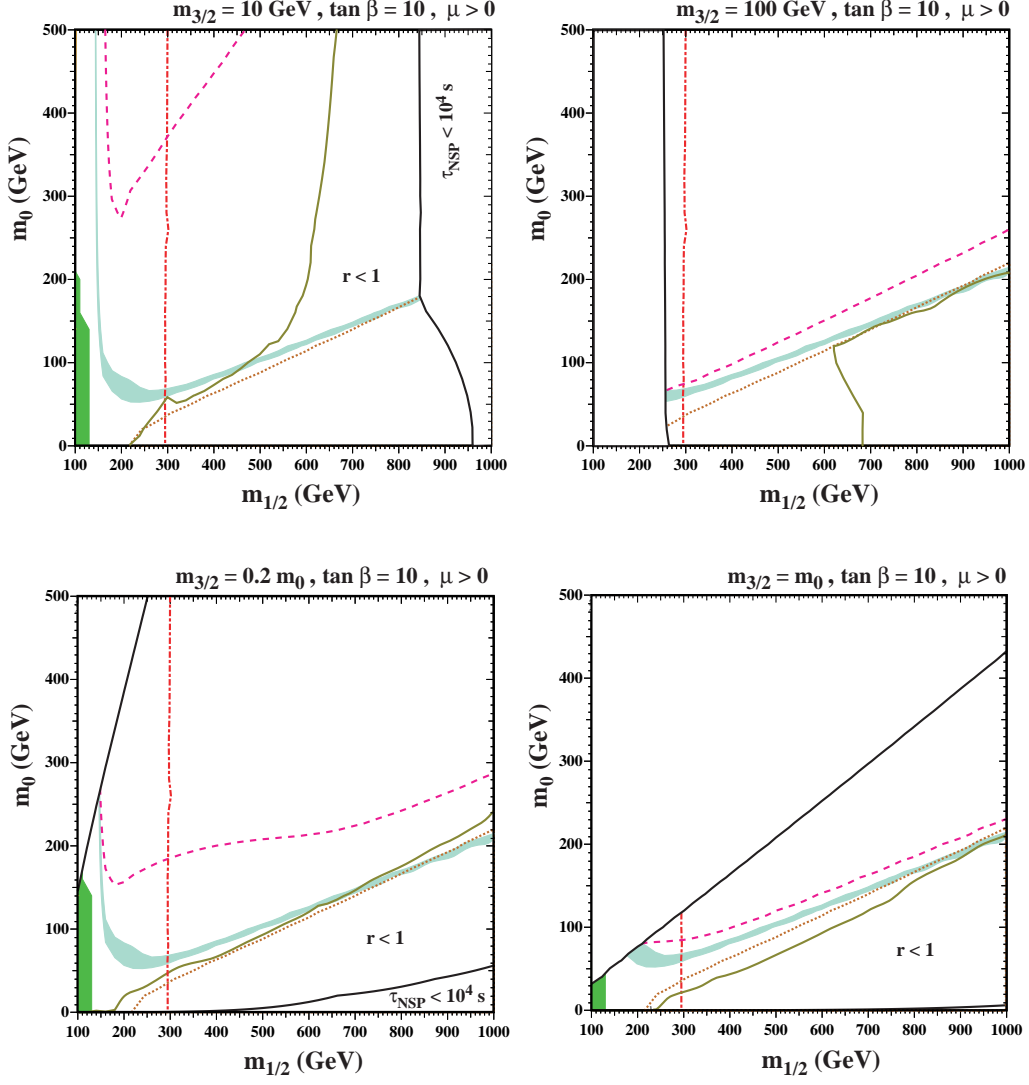


Figure 1: The  $(m_{1/2}, m_0)$  planes for  $\tan \beta = 10, \mu > 0$  and the choices (a)  $m_{3/2} = 10 \text{ GeV}$ , (b)  $m_{3/2} = 100 \text{ GeV}$ , (c)  $m_{3/2} = 0.2 m_0$  and (d)  $m_{3/2} = m_0$ . In each panel, we show  $m_h = 114 \text{ GeV}$  calculated using **FeynHiggs** [24], as a near-vertical (red) dot-dashed line, the region excluded by  $b \rightarrow s\gamma$  is darkly shaded (green), and the region where the NSP density before decay lies in the range  $0.094 < \Omega_{NSP}^0 h^2 < 0.129$  is lightly shaded (turquoise). The (purple) dashed line is the contour where gravitinos produced in NSP decay have  $\Omega_{3/2} h^2 = 0.129$ , and the grey (khaki) solid line ( $r = 1$ ) is the constraint on NSP decays provided by Big-Bang nucleosynthesis and CMB observations. The contour where  $m_\chi = m_{\tilde{\tau}_1}$  is shown as a (red) diagonal dotted line. Panels (a) and (c) show as a black solid line the contour beyond which  $\tau_{NSP} < 10^4 \text{ s}$ , the case not considered here. Panels (b), (c), and (d) show black lines to whose left the gravitino is no longer the LSP.

Finally, in panel (d) of Fig. 1, where now  $m_{3/2} = m_0$ , the  $\tilde{G}$  constraint is more powerful, as is the  $\Omega_{3/2}h^2$  constraint, and the region finally allowed by the light-element constraint on NSP decays is again in the  $\tilde{\tau}_1$  region.

Fig. 2 displays a similar array of  $(m_{1/2}, m_0)$  planes for the case  $\tan\beta = 35$  and  $\mu < 0$ . In the case where  $m_{\tilde{\tau}_1} = 10$  GeV, shown in panel (a), the most significant change compared with panel (a) of Fig. 1 is that the  $b \rightarrow s\gamma$  constraint is more important, whilst the  $\Omega_{3/2}h^2$ , NSP decay and  $\tau_{NSP}$  constraints do not change so much. The net result is to leave disconnected parts of both the  $\chi$  and  $\tilde{\tau}_1$  regions that are allowed by all the constraints.

The most obvious new feature in panel (b) of Fig. 2 is the rapid-annihilation funnel, which affects both the  $\Omega_{3/2}h^2$  and NSP decay constraints. The former acquires a strip extending to large  $m_{1/2}$  and  $m_0$ , whereas the latter would have allowed a region at large  $m_{1/2} \gtrsim 1500$  GeV that is excluded by  $\Omega_{3/2}h^2$ . Combining this and the NSP decay constraint, we again find two disconnected allowed regions, one in the  $\chi$  NSP region and one that is almost entirely in the  $\tilde{\tau}_1$  NSP region.

The rapid-annihilation funnel is also very apparent in panel (c) of Fig. 2, which displays the case  $m_{\tilde{\tau}_1} = 0.2m_0$ , where again a strip allowed by both the  $\Omega_{3/2}h^2$  and NSP decay constraints extends to large  $m_{1/2}$  and  $m_0$ . There are again disconnected allowed regions in the  $\chi$  and (mainly) the  $\tilde{\tau}_1$  NSP region. Note that this is constrained at large  $m_{1/2}$  and small  $m_0$  by the  $\tau_{NSP}$  constraint. Finally, in panel (d) of Fig. 2, for  $m_{\tilde{\tau}_1} = m_0$ , the region allowed by the  $\tilde{G}$  LSP,  $\Omega_{3/2}h^2$  and NSP decay constraints is restricted to the part of the  $(m_{1/2}, m_0)$  plane where the  $\tilde{\tau}_1$  is the NSP.

Fig. 3 displays a similar array of  $(m_{1/2}, m_0)$  planes for the case  $\tan\beta = 50$  and  $\mu > 0$ . The general features of the planes have some similarities to those for  $\tan\beta = 35$  and  $\mu < 0$ . There are differences in the interplays between the  $\Omega_{3/2}h^2$  and NSP decay constraints, but an important difference is the relative weakness of the  $b \rightarrow s\gamma$  constraint. This has the consequence that allowed  $\chi$  and  $\tilde{\tau}_1$  regions are connected for  $\tan\beta = 50$  and  $\mu > 0$ . It is interesting to note that this is the only case where the putative constraint imposed by the muon anomalous magnetic moment  $a_\mu$  impinges on the allowed region, as shown in panels (a) and (c).

We have seen in the above examples that many of the allowed parts of the  $(m_{1/2}, m_0)$  planes are confined to regions where the NSP is the  $\tilde{\tau}_1$ .

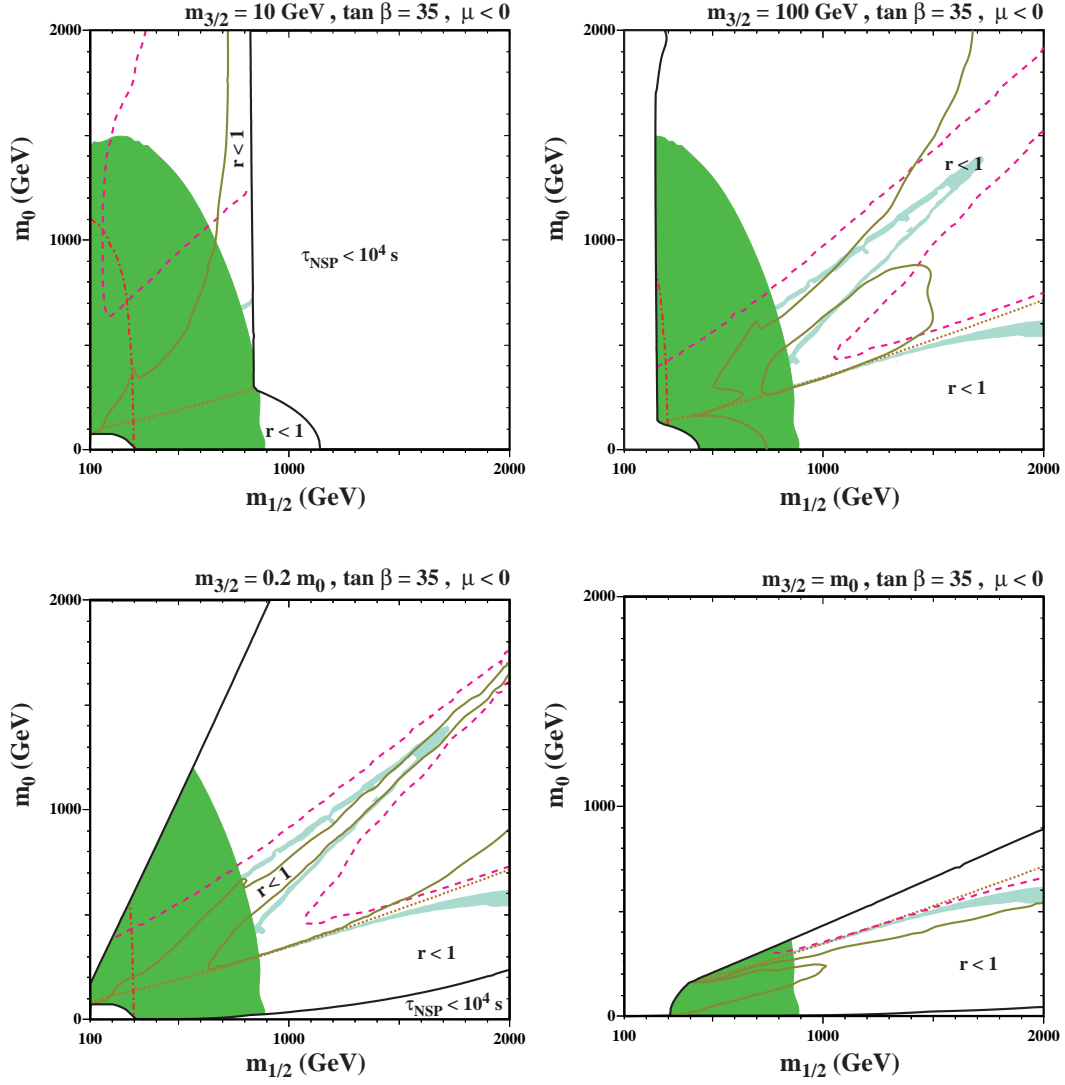


Figure 2: As in Fig. 1, for  $\tan \beta = 35$  and  $\mu < 0$  and the choices (a)  $m_{3/2} = 10 \text{ GeV}$ , (b)  $m_{3/2} = 100 \text{ GeV}$ , (c)  $m_{3/2} = 0.2 m_0$  and (d)  $m_{3/2} = m_0$ .

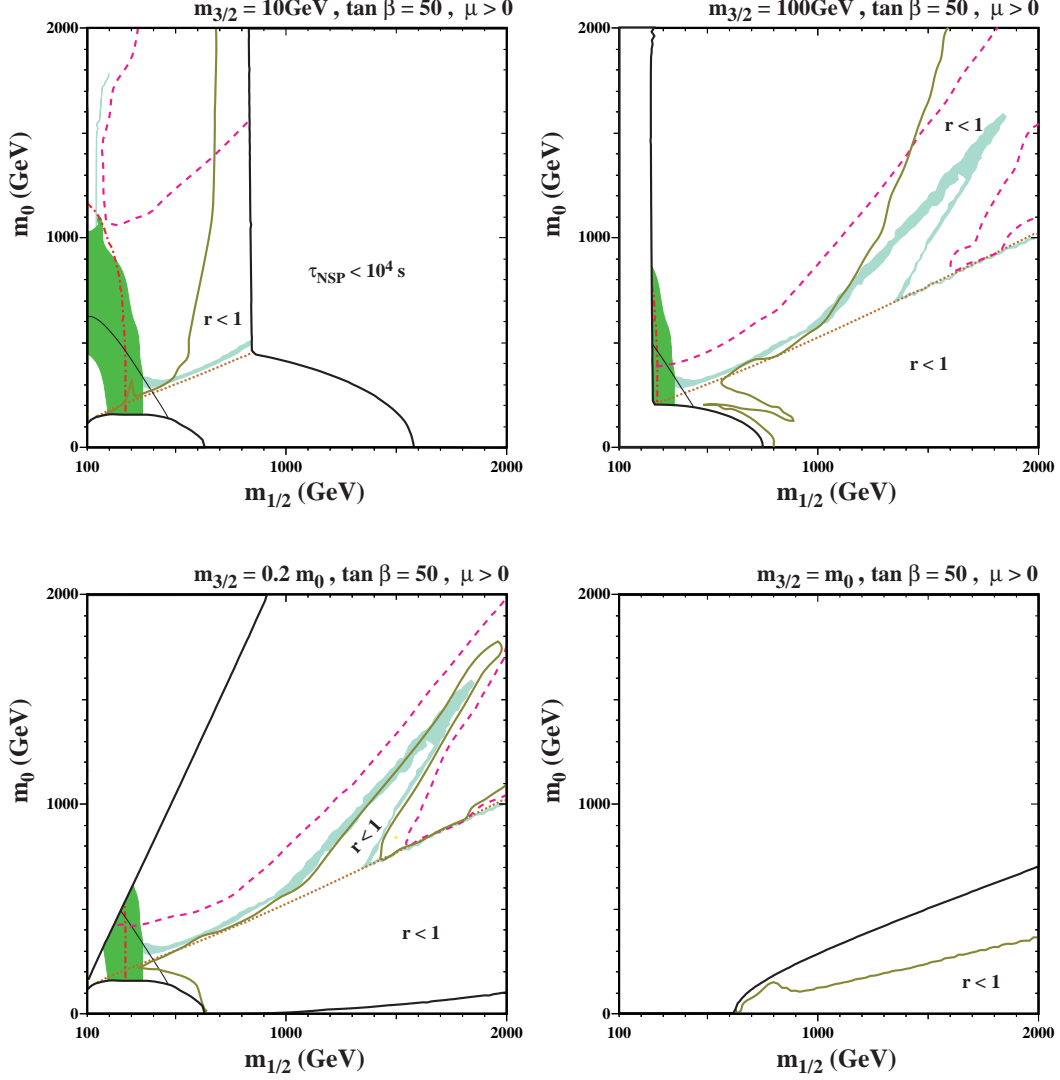


Figure 3: As in Figs. 1 and 2, for  $\tan \beta = 50$  and  $\mu > 0$  and the choices (a)  $m_{3/2} = 10 \text{ GeV}$ , (b)  $m_{3/2} = 100 \text{ GeV}$ , (c)  $m_{3/2} = 0.2 m_0$  and (d)  $m_{3/2} = m_0$ . In addition to the quantities plotted in the earlier figures, here we also plot grey solid lines where  $a_\mu = 44.5 \times 10^{-10}$ , which cut off at small  $m_0$  the allowed regions in panels (a) and (c).

## 6 Conclusions

We have analyzed in this paper the possibility of gravitino cold dark matter within the CMSSM framework. Combining accelerator and cosmological constraints, particularly those from  $b \rightarrow s\gamma$ ,  $\Omega_{3/2}h^2$  and the light-element constraint on NSP decays, we have found allowed regions in the  $(m_{1/2}, m_0)$  planes for representative values of  $\tan\beta$  and the sign of  $\mu$  and different values of  $m_{3/2}$ . Standard calculations of the NSP density before decay based on freeze-out from equilibrium yield allowed regions where either the lightest neutralino  $\chi$  or the lighter stau  $\tilde{\tau}_1$  may be the NSP.

One limitation of our analysis is that it is restricted to  $\tau_{NSP} > 10^4$  s, in order to avoid issues related to the hadronic interactions of NSP decay products before they decay. Also, in this paper we have not discussed at much length what part of parameter space may be allowed in the focus-point region. Finally, we have analyzed here only a few examples of the possible relationship between  $m_{3/2}$  and the CMSSM parameters  $m_0$  and  $m_{1/2}$ .

For these and other reasons, there are still many important issues to analyze concerning the possibility of gravitino dark matter. We have shown in this paper that such a possibility certainly exists, and that the allowed domains of parameter space are not very exceptional. We consider that gravitino dark matter deserves more attention than it has often received in the past. In particular, this possibility should be borne in mind when considering the prospects for collider experiments, since the allowed regions of the  $(m_{1/2}, m_0)$  are typically rather different from those normally analyzed in the CMSSM. *Vive la différence!*

### Acknowledgments

We would like to thank Rich Cyburt for providing us with BBN analysis data, and Stefan Groot Nibbelink for helpful conversations. Y.S. would like to thank Richard Arnowitt for useful discussions. We would also like to thank Koichi Hamaguchi for constructive comments regarding the original version of the manuscript. The work of K.A.O., Y.S., and V.C.S. was supported in part by DOE grant DE-FG02-94ER-40823.

## References

- [1] J. Ellis, J.S. Hagelin, D.V. Nanopoulos, K.A. Olive and M. Srednicki, Nucl. Phys. B **238** (1984) 453; see also H. Goldberg, Phys. Rev. Lett. **50** (1983) 1419.
- [2] J. R. Ellis, J. E. Kim and D. V. Nanopoulos, Phys. Lett. B **145** (1984) 181.

- [3] T. Moroi, H. Murayama and M. Yamaguchi, Phys. Lett. B **303** (1993) 289.
- [4] J. R. Ellis, D. V. Nanopoulos, K. A. Olive and S. J. Rey, Astropart. Phys. **4** (1996) 371 [arXiv:hep-ph/9505438].
- [5] M. Bolz, W. Buchmuller and M. Plumacher, Phys. Lett. B **443** (1998) 209 [arXiv:hep-ph/9809381].
- [6] T. Gherghetta, G. F. Giudice and A. Riotto, Phys. Lett. B **446** (1999) 28 [arXiv:hep-ph/9808401]; T. Asaka, K. Hamaguchi and K. Suzuki, Phys. Lett. B **490** (2000) 136 [arXiv:hep-ph/0005136]; M. Fujii and T. Yanagida, Phys. Rev. D **66** (2002) 123515 [arXiv:hep-ph/0207339]; Phys. Lett. B **549** (2002) 273 [arXiv:hep-ph/0208191].
- [7] M. Bolz, A. Brandenburg and W. Buchmuller, Nucl. Phys. B **606** (2001) 518 [arXiv:hep-ph/0012052].
- [8] . L. Feng, A. Rajaraman and F. Takayama, Phys. Rev. Lett. **91** (2003) 011302 [arXiv:hep-ph/0302215]; Phys. Rev. D **68** (2003) 063504 [arXiv:hep-ph/0306024].
- [9] R. H. Cyburt, J. R. Ellis, B. D. Fields and K. A. Olive, Phys. Rev. D **67** (2003) 103521 [arXiv:astro-ph/0211258].
- [10] C. L. Bennett *et al.*, Astrophys. J. Suppl. **148** (2003) 1 [arXiv:astro-ph/0302207].
- [11] J. R. Ellis, K. A. Olive and Y. Santoso, New Jour. Phys. **4** (2002) 32 [arXiv:hep-ph/0202110].
- [12] V. D. Barger and C. Kao, Phys. Lett. B **518** (2001) 117 [arXiv:hep-ph/0106189]; L. Roszkowski, R. Ruiz de Austri and T. Nihei, JHEP **0108** (2001) 024 [arXiv:hep-ph/0106334]; A. B. Lahanas and V. C. Spanos, Eur. Phys. J. C **23** (2002) 185 [arXiv:hep-ph/0106345]; A. Djouadi, M. Drees and J. L. Kneur, JHEP **0108** (2001) 055 [arXiv:hep-ph/0107316]; U. Chattopadhyay, A. Corsetti and P. Nath, Phys. Rev. D **66** (2002) 035003 [arXiv:hep-ph/0201001]; H. Baer, C. Balazs, A. Belyaev, J. K. Mizukoshi, X. Tata and Y. Wang, JHEP **0207** (2002) 050 [arXiv:hep-ph/0205325]; R. Arnowitt and B. Dutta, arXiv:hep-ph/0211417; J. R. Ellis, K. A. Olive, Y. Santoso and V. C. Spanos, Phys. Lett. B **573** (2003) 163 [arXiv:hep-ph/0308075].
- [13] J. R. Ellis, K. A. Olive, Y. Santoso and V. C. Spanos, Phys. Lett. B **565** (2003) 176 [arXiv:hep-ph/0303043].

- [14] H. Baer and C. Balazs, JCAP **0305** (2003) 006 [arXiv:hep-ph/0303114]; A. B. Lahanas and D. V. Nanopoulos, Phys. Lett. B **568** (2003) 55 [arXiv:hep-ph/0303130]; U. Chattopadhyay, A. Corsetti and P. Nath, Phys. Rev. D **68** (2003) 035005 [arXiv:hep-ph/0303201]; C. Munoz, arXiv:hep-ph/0309346; R. Arnowitt, B. Dutta and B. Hu, arXiv:hep-ph/0310103.
- [15] see e.g., A. Brignole, L. E. Ibanez and C. Munoz, arXiv:hep-ph/9707209; R. Arnowitt and P. Nath, arXiv:hep-ph/9708254.
- [16] C. Boehm, A. Djouadi and M. Drees, Phys. Rev. D **62** (2000) 035012 [arXiv:hep-ph/9911496]; J. R. Ellis, K. A. Olive and Y. Santoso, Astropart. Phys. **18** (2003) 395 [arXiv:hep-ph/0112113].
- [17] J. R. Ellis, T. Falk, G. Ganis, K. A. Olive and M. Srednicki, Phys. Lett. B **510** (2001) 236 [arXiv:hep-ph/0102098].
- [18] E. Cremmer, S. Ferrara, L. Girardello and A. Van Proeyen, Nucl. Phys. B **212** (1983) 413.
- [19] J. Wess and J. Bagger, *Supersymmetry and Supergravity*, Princeton University Press, New Jersey 1992; T. Moroi, arXiv:hep-ph/9503210.
- [20] M. H. Reno and D. Seckel, Phys. Rev. D **37** (1988) 3441; S. Dimopoulos, R. Esmailzadeh, L. J. Hall and G. D. Starkman, Nucl. Phys. B **311** (1989) 699; K. Kohri, Phys. Rev. D **64** (2001) 043515 [arXiv:astro-ph/0103411].
- [21] M. Drees and M. M. Nojiri, Phys. Rev. D **47** (1993) 376 [arXiv:hep-ph/9207234]; H. Baer and M. Brhlik, Phys. Rev. D **53** (1996) 597 [arXiv:hep-ph/9508321]; A. B. Lahanas, D. V. Nanopoulos and V. C. Spanos, Phys. Rev. D **62** (2000) 023515 [arXiv:hep-ph/9909497]; Mod. Phys. Lett. A **16** (2001) 1229 [arXiv:hep-ph/0009065]; H. Baer, M. Brhlik, M. A. Diaz, J. Ferrandis, P. Mercadante, P. Quintana and X. Tata, Phys. Rev. D **63** (2001) 015007 [arXiv:hep-ph/0005027].
- [22] K. L. Chan, U. Chattopadhyay and P. Nath, Phys. Rev. D **58** (1998) 096004 [arXiv:hep-ph/9710473].
- [23] J. L. Feng, K. T. Matchev and T. Moroi, Phys. Rev. Lett. **84** (2000) 2322 [arXiv:hep-ph/9908309]; J. L. Feng, K. T. Matchev and T. Moroi, Phys. Rev. D **61** (2000) 075005 [arXiv:hep-ph/9909334]; J. L. Feng, K. T. Matchev and F. Wilczek, Phys. Lett. B **482** (2000) 388 [arXiv:hep-ph/0004043].

- [24] S. Heinemeyer, W. Hollik and G. Weiglein, Comput. Phys. Commun. **124** (2000) 76 [arXiv:hep-ph/9812320]; S. Heinemeyer, W. Hollik and G. Weiglein, Eur. Phys. J. C **9** (1999) 343 [arXiv:hep-ph/9812472].